<u>STRUCTURES SUBSYSTEM FINAL DESIGN REPORT</u>
2001-2002

Project Director:
Dan Coyle

Structures Subsystem Team (2001-2002):

Chris Wilkening
Raymond Yang
Adrianne Kelly
Risela
Anthony

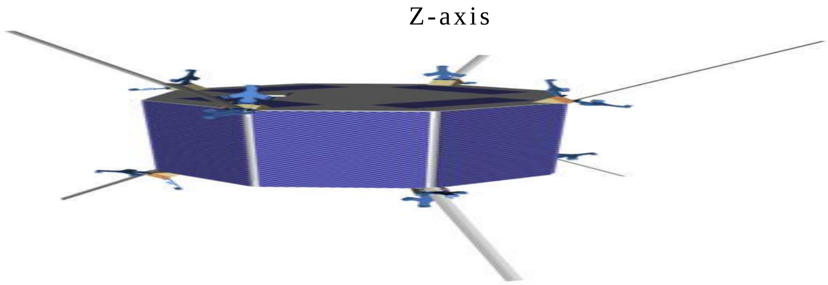

Projected Assembled Spartnik Structure
Width = 17.109
Height = 12.383

Table of Contents

List of Figures

List of Tables

Introduction

The primary responsibility of the structures team was to design and build a structure (hereafter called Spartnik) that provided: the skeletal framework for attaching all subsystems, subsystem protection from the space environment, and the structural rigidity to withstand all anticipated loads with a high margin of safety. The secondary objectives included design considerations such as thermal conduction paths, subsystem placement for proper mass distribution and moments of inertia, and payload placement for best earth viewing. The Final Design Report (FDR) summarizes all the structural work done from establishing requirements to actual manufacturing and environmental qualification testing.

The following drawings are excerpts from actual CAD drawings done by team members. They are designed to familiarize the reader with Spartnik and the Launch Vehicle Adapter (LVA) it uses to mount to the secondary payload bay of the launch vehicle. The LVA will be covered first.

3.1.0 Launch Vehicle Adapter

Figure 3.1: Exploded View of Launch Vehicle Adapter

The launch vehicle adapter (LVA), Fig. 3.1, is the interface between the launch vehicle and Spartnik. It secures Spartnik to the launch vehicle during launch. Upon reaching the predetermined orbit, the LVA receives a signal from the launch vehicle to activate the release mechanism. Once activated, a spring deploys Spartnik away from the launch vehicle.

The LVA is made up of 12 main components:

1. Launch Vehicle Adapter Plate
2. Stand-off Plates (x3)
3. Non-explosive Release Mechanism
4. Release Mechanism Plate
5. Baseplate Hub/Seat
6. Deployment Spring (x1) and Retaining Clips (x2)
7. Satellite Baseplate
8. Main Bolt

Launch Vehicle Adapter Plate

The launch vehicle adapter plate bolted to the launch vehicle, accommodates the firing mechanism wiring, and attaches the stand-off plates. The plate is 5/8-inch thick solid aluminum 6061-T6 with through holes for bolting to the launch vehicle, and counter-bored holes on the bottom for securing the stand-off plates. This part remains with the launch vehicle after Spartnik separates.

Stand-off Plates

The stand-off plates are the three components that bolt to the launch vehicle adapter plate by four ¼-20 socket head cap screws, each. Their purpose is to provide the structural support and interface between the launch vehicle adapter plate and the satellite baseplate. The standoff plates have steel helical inserts for all tapped holes to increase pull out strength and to allow many assembly/disassembly cycles of the structure without destroying the insert threads. The stand-off plates serve four purposes:

1. A mounting platform for the separation mechanism
2. Provides adequate space between the launch vehicle and the satellite for deployment hardware: non-explosive actuator, bolt shaft, spring
3. Act as part of the bearing surface for the satellite baseplate
4. Aid in restraining Spartnik from lateral motion through contact with the protruding truncated cone of the satellite baseplate and the 120^{0} surface

Release Mechanism Plate

This plate will hold the release actuator to the stand-off plates, which also connects all three stand-off plates together for structural stability. The plate is made of aluminum 6061-T6. This part also remains with the launch vehicle after satellite separation.

Baseplate Hub/Seat

The central baseplate Hub/Seat serves two purposes: stiffening the stand-off members in the X-Y plane to reduce strains due to torsion; provide an additional cup and cone restraint to lateral motion while preserving the freedom required for deployment release.

The hub is made of 6061-T6 aluminum and is centrally bored out with a 1.25-inch diameter hole to accommodate the deployment spring and retaining clips. The hub structure remains with the launch vehicle after satellite deployment.

Satellite Baseplate

The satellite baseplate is the mounting plate for the satellite. The satellite attaches to the baseplate via the four threaded rods that extend through the satellite structure. The baseplate is square, 8.485-inches per side; made of 0.438 thick, 6061-T6 aluminum. The baseplate remains after separation.

Satellite Baseplate Features:

1. It will act as a radiator by conducting heat from the bottom of the satellite out to the high emmissivity FOSR (Flexible Optical Surface Radiator) material.
2. It will block solar radiation from heating the underside of the satellite (FOSR is applied to the bottom side of the baseplate).
3. Act as the truncated cone of the "cup and cone" design to prevent lateral motion and ensure un-obstructed separation from the launch vehicle.
4. Transfers and distributes heat and loads to and from the four structural members of the satellite.
5. Houses the main bolt that keeps that satellite attached to the release mechanism before separation
6. Houses the three power-up switches used to initiate the power-up sequence after tip off.

Main Bolt

The main bolt is a ¼-28 UNF Grade 8 Steel bolt plated with gold alodine to prevent corrosion. The main bolt is 3.375-inches long and is torqued into the release mechanism to 100 in-lbf. This preloads the release mechanism and bolt to approximately 2500 lbf. The bolt should not be torqued any more than this since the added mass of the spacecraft and the loads it will experience during launch may cause a structural failure of the release mechanism.

Possible Modifications to the LVA

With the elimination of the hysteresis rods and solar pressure panels (see ADAC papers for a discussion of the underlying reasons) Spartnik is left with out a spin up or spin control mechanism. It has been proposed that modifications be made to the LVA so that it will provide a one time spin up during re release. The leading method of altering the LVA would involve using a torsional as well as compressive spring. This would involve minimal macroscopic changes to the overall design of the LVA. Further notes on the modifications proposed can be found in the "big book" with in the IM section.

Individual tray components provide subsystem level modularity and ease of integration.
The spacers are spool-like cylinders providing structural support and thermal conduction paths to minimize thermal gradients across the satellite.

Figure 3.3: Modular Tray Unit (with Spacers and "notional" subsystem)

3.1.1 Design Summary

This section of the Final Design Report (FDR) addresses the various mission requirements and constraints and how they drove the structural design, and hence the final design.

3.1.2 Launch Vehicle Requirements

Limited funding drove this project to innovate and, unlike most projects, to the additional need for a donated launch. This in turn placed additional design constraints on Spartnik and the Launch Vehicle Adapter to accommodate as many launch vehicles as possible.

Each launch vehicle has its own unique launch profile and secondary payload bay requirements. In general, thrust (axial) loads range between 8 to 12 Gs while acoustic loads can reach up to 120 Gs at specific frequencies. Initial modeling of Spartnik (to include the shell, spacers and spools, but no LVA) was accomplished using a geometric element-modeling program called Mechanica, by Parametric Technologies (now Pro/Mechanica). Due to

Top Plate

*Note: The positive Z face is surface 9 and the negative Z face is surface 10.

the limited

Figure 32: Spartnik Satellite (

Camera Box

Shell

Spacers

Payload Tray

Power Subsystem

Battery boxes

Hysteresis Rods (eliminated)

Spacers

Computer/Communications Subsystem

Computer/Communications Tray

Launch Vehicle Adapter

computing power of SJSU's workstations, meshing of the structure was accomplished free of charge through contacts at Parametric Technologies. The final as-built structure was also modeled in Mechanica; unfortunately, our free access to the more powerful computers at Parametric Technologies no longer existed. Thus, our mentor, Eric Abrahamson, volunteered to build and model the structure using ABAQUS, a commercial finite element code he uses at SC Solutions. Results of his modeling are covered in a subsequent section.

Each launch vehicle has its own space allocation for secondary payloads along with its unique secondary Launch Vehicle Adapter (LVA) requirements. A bulkhead-adaptable LVA has been built for Spartnik. The spring release mechanism (donated by G&H Technologies) provides the means for deployment from the launch vehicle. The entire LVA has undergone qualification and acceptance shake testing both with and without Spartnik attached.

3.1.3 Booster Loads

The first phase of the launch profile is the boost phase. During boost, the satellite will undergo axial acceleration loads of 8 to 12 Gs and acoustic loads of 40 to 50 Gs, sometimes reaching as high as 130 Gs.[1,2] This load is generated by random vibration from the engines. During powered flight, rocket engines produce sound pressure waves that far exceed the loads produced by thrust. Fortunately these vibration loads occur only at certain frequencies. If these frequencies coincide with Spartnik's natural frequencies, the satellite could "rip" itself apart from the high-induced resonance; thus, frequency analysis of the structure is vital. Shake tests of the LVA and Spartnik will determine the natural frequencies. For most launch vehicles, the maximum displacements due to vibration are associated with frequencies below 100 Hz.

3.1.3.1 Axial Loads

Thrust loads range from 8 to 12 Gs and load Spartnik along its stiffest design axis, the z-axis. Lateral loads of 2 to 5 Gs due to wind buffering and transonic buffering are not uncommon and, unfortunately, not predictable. Even though cantilevered from the bulkhead in the secondary payload bay, LVA/Spartnik is braced internally across its width for lateral loads. Nevertheless, loads along each axis are analyzed for resonant frequencies during the 0.5G sinusoidal shake tests, and for maximum displacement and stress during the 14G random vibration tests. Results show that LVA/Spartnik combination is a very stiff structure, capable of withstanding anticipated launch loads.

3.1.3.2 Shock Loads

Shock loads include events like rocket engine ignition or stage separation. The shock environment can be sudden and severe. Loads can reach 2000 Gs but last only milliseconds. The table below summarizes these loads.

Table 3.1: Peak Shock Loads

Launch Vehicle	Peak Load Frequency (Hz)	Shock Loads (G)
Pegasus	1000 and above	200
Ariane IV	1500 and above	2000
LMLV3	1500	15
STS	31	50

The peak load frequencies indicate the launch vehicle's first mode of resonance, the mode with the potentially highest amplitude of induced oscillation. Obviously, these loads are too large to design for; they must be avoided. From the data, Pegasus's peak load frequency is the lowest or limiting frequency. Using a 10% error bar, 900 Hz becomes the self-imposed limiting frequency for design purposes. Spartnik's shake test results indicate that its first two (i.e. most significant amplitude) modes occur at the resonant frequencies of 65 Hz and 245 Hz. Thus, Spartnik's resonant modes do not approach that of any of the vehicles. This is an important design consideration but not the only one. Acoustic loads can also impart high G resonance within the spacecraft if not taken in to account.

3.1.3.3Acoustic (Transient) Loads

Acoustic loads vary widely by vehicle. The acoustic environment generates random vibration loads due to the sound pressure acting on the surfaces of the spacecraft.[3] Acoustic loads are developed during powered ascent, the first 3 to 4 minutes of ascent. Compression waves are particularly significant for structures with a ratio of high cross-sectional area to low mass.[3] Solar panels are an excellent example of a structure with high specific area. Structures with high specific area inherently have low stiffness and are subject to damage.

Just as significant is the possibility that the satellite has a mode or natural frequency that is the same as that generated by the launch vehicle. These loads are significant from frequencies of 20 Hz to well over 1000 Hz. These ranges and loads are calculated from a Power Spectral Density chart, which is documented by the launch vehicle manufacturer.[4,5,6,7] An example of this process is shown using the Pegasus launch vehicle (Figure 3.4). Geometric Element Modeling predicted Spartnik's natural frequencies, which, along with vibration tests, were well correlated. Spartnik's modes differed from the launch vehicles' frequency modes.

Figure 3.4: Pegasus Power Spectral Density Chart

This chart can be translated to acceleration as a function of frequency using the following equation:

(3-1)

Reference: Fundamentals of Space Systems. Pisacane, Vincent L. and Robert C. Moore. Editors. Oxford University Press, New York. 1994

where,

G = acceleration (G)
f = frequency (Hz)
Q = Amplification Factor (10)

S_o = Power Spectral Density (G^2 /Hz)

Table 3.2: Pegasus Acceleration Values

2000	0.001	16.81

These acceleration values were then plotted versus frequency to obtain the graph in Figure 3.5 (fitted curve).

Figure 3.5: Pegasus Acceleration

Using this formula, vibration load graphs were generated for all the launch vehicles (see Appendix 3.A). The peak loads are summarized below:

Table 3.3: Peak Acoustic Loads

Launch Vehicle	Peak Load Frequency (Hz)	Acoustic Loads (G)
Ariane IV	500-2000 (inclusive)	119
Pegasus	1400	121.8
LLV3	1000	141
STS	600	77.1

These loads are typical of random acoustic loads generated in all three axes. Luckily, designing a structure to withstand a 120 G load is not necessary. These loads occur over a range of frequencies, which are well defined. It is the task of the designer to keep the natural frequency of the structure in a range that will prevent the stresses produced by the acoustic launch loads from approaching the yield strength of the structure. Following is a general list of various launch vehicles showing various load environments.

3.1.4 Payload Accommodations[17]

Ariane 4

Maximum Load Factors:	+4.5 g axial, 0.2 g lateral
Minimum Lateral / Longitude Payload Frequency:	10 Hz / 31 Hz
Maximum Flight Shock:	2,000 g from 1,500 – 4,000 hz

Ariane 5

Maximum Load Factors:	+4.5 g axial, ?? g lateral
Minimum Lateral / Longitude Payload Frequency:	?? Hz / ?? hz
Maximum Flight Shock:	?? g at ?? Hz

Titan II

Maximum Load Factors:	+4.0 to +10.0 g axial, 2.5 g lateral
Minimum Lateral / Longitude Payload Frequency:	2 – 10 Hz avoid <6 Hz / 12 – 24 Hz
Maximum Flight Shock:	200 g at 500 Hz

Titan III

Maximum Load Factors:	+2.5, -5.0 g axial, 1.7 g lateral
Minimum Lateral / Longitude Payload Frequency:	10 Hz / 26 Hz
Maximum Flight Shock:	4,100 g at 1,250 Hz

Titan IV

Maximum Load Factors:	+3.3, -6.5 g axial, 1.5 g lateral
Minimum Lateral / Longitude Payload Frequency:	>2.5 Hz avoid 6 - 10 Hz / 17 –24 Hz
Maximum Flight Shock:	2,000 g at 5,000 Hz

Delta II

Maximum Load Factors:	+6.0 g axial, 2.0 g lateral
Minimum Lateral / Longitude Payload Frequency:	15 Hz / 35 Hz

Maximum Flight Shock: 5,500 g at 4,000 hz for 2 stage vehicle
4,100 g at 1,500 hz for 3 stage vehicle

Proton

Maximum Load Factors: +3.65 g axial, 1.5 g lateral
Minimum Lateral / Longitude Payload Frequency: 15 Hz / 30 Hz
Maximum Flight Shock: 2,000 g from 1,500 – 5,000 hz, typical value during payload separation

3.1.5 Orbit Requirements

The second design phase depends on orbit. This phase begins when the satellite deploys from the launch vehicle upon reaching orbit. The mission life objective for Spartnik is a minimum of two years on-orbit. To reach this lifetime goal, many factors must be considered. The structure must have sufficient surface area to accommodate the number of solar cells required to generate the necessary power to support ongoing operations, and to charge the batteries (while exposed to the sun). Insufficient battery charging per orbit cycle quickly leads to progressively larger depths of discharge on the batteries – this in turn reduces mission life quite rapidly (less than two years). The structure must also protect the payloads from harmful radiation, micrometeorite impacts, as well as survive the thermal cycling that the sun-eclipse cycle will impart on the structure itself.

3.2 Design

In the initial design, Spartnik's main structure comprised the largest percentage mass of all the subsystems. A robust yet lightweight design is critical. In order to achieve such a design goal, shrewd material choices would make the difference.

When the design process began, 1/8-inch thick solid aluminum 6061-T6 plate stock was considered for the design. Preliminary research showed that many large satellite producers use Al 6061-T6 or 7075 for the framework of the satellite bus, in conjunction with Aluminum honeycomb paneling for the walls.

Initial mass studies showed the solid aluminum plate structure was over 17 kg for the basic structure nearly one-third of the overall budget (50 kg). Since solid aluminum was far too massive, aluminum honeycomb was chosen (Figure 3.6). Note that the final structure with Honeycomb panels and Aluminum spacers weighed approximately 17 kg when assembled.

Figure 3.6: Structure Mass vs. Material

3.2.1 Material Selection

The primary structural material chosen was aluminum honeycomb, the highest specific strength of the most readily available materials studied. Higher specific strength materials like carbon-based composites were considered early in the design, but high cost, limited availability, and special tooling requirements ruled out this option.

3.2.2 Material Properties

Aluminum honeycomb sandwich structure is known for its high stiffness and low mass. Honeycomb sandwich panels allow for a seven-fold increase in stiffness, an over three-fold increase in strength, and a minuscule weight gain simply by doubling the thickness of the panel relative to a solid plate of aluminum.[8]

The primary benefit of honeycomb panels is the manner in which loading is distributed. The sandwich panel accepts a load, and transmits the load through the core to the face sheets. This allows the panel to resist the loading in shear only, and increases the stiffness since all the loads are translated into the plane of the face sheet.[10] The rigid joint between the core and the facing sheets allows the panel to function as a unit with high torsion and bending stiffness.

This means that the majority of the shear forces are transmitted through the core and taken up within the facings. So it is important to consider facing thickness and core type when selecting a sandwich structure. The thicker the core the stiffer the panel, and conversely in order to maintain adequate stiffness in thinner panels, a higher density core is needed as well as thicker facing sheets.

The relationship of core type and facing thickness is clear. A proper combination must be found in order to satisfy the structural load requirements of the satellite. Using the physical properties of the materials, a series of trade studies were conducted to investigate the

Figure 3.7: Structure Mass vs. Aluminum Honeycomb Facing Material & Thickness

Relationship between satellite mass and the type of sandwich structure used. Figure 3.7 shows the increase in structural mass as the thickness of the facing sheets is increased. It is seen that depending on required thickness, the structural mass can vary widely from below 1 kilogram to over 9 kilograms.

Further studies were conducted comparing core type and its effect on mass shown in Figure 3.8 and Figure 3.9. Its effect on overall mass is considerably less significant compared to the facing thickness (the core study was modeled with 0.020 inch thick facing sheets).

Figure 3.8: Honeycomb Mass as a Function of Core Type Aluminum 5056 Hexagonal

Figure 3.9: Honeycomb Mass as a Function of Core Type Aluminum 5052 Hexagonal

Depending on the core material, cell size, and cell thickness combination, the core only varied the total mass by a margin of around 2 kg (4.4 lb_m) for either Al 5052 or Al 5056. These preliminary trade studies provide some clarity for future investigations. The figures clearly show that the Al 6061-T6 facing and Al 5056 core combination is the optimum baseline choice for their respective function. Al 6061-T6 is chosen for its higher strength and its lower weight compared to the other facing choice of Al 2024-T3. Due to the fact that 5052 and 5056 are practically identical in mass characteristics, Figure 3.9 also indicates that 5056 is the preferred choice because of its greater shear strength. In addition to their stiffness and toughness, the panels should provide a modicum of radiation shielding, micrometeorite impact absorption, and thermal insulation.

Initial cost estimates for this Aluminum honeycomb averaged around $1000 per sheet (48" x 80" x 1/2"). Fortunately, TEKLAM was gracious enough to donate aluminum honeycomb under the stipulation that all material was chosen from stock-on-hand. However, stock-on-hand did not include 6061-T6 (facing sheets) or 5056 (core). The final material choice of 2024-T3 face sheet and 5052 honeycomb was similar in performance to our optimum choice.

In particular, the actual panels are a hexagonal honeycomb sandwich construction (1/2 inch thick). The core (1/4 cell size) is made of Al 5056 perforated honeycomb ((0.0015" gage) and the facing sheets of Al 2024-T3 (0.020" thick). The sandwich is constructed by combining the layers together using space rated epoxy[8]. As noted earlier, the entire structure will be made of these panels, including the top and bottom plates and interior shelves.

3.2.3 Spartnik Structure

The spacecraft structure consists of an outer, regular octahedral shell with octagonal top and bottom faces attached with a total of 16 angle brackets, one at each vertex. Four alloy steel rods run through the entire assembly providing structural integrity (Figure 3.10). The rods keep the shelves aligned during the launch and provide mount points for the

Figure 3.10: Structural Members of Spartnik

Launch Vehicle Adapter. 4130 Alloy Steel is the material of choice. This steel has the right characteristics to satisfy our design constraints. We have coated the rods with a silver coating to ensure corrosion resistance. The rods are sheathed by aluminum spacers which serve to support not only the shelves carrying the subsystem components but act as heat conduction paths through the structure, thereby minimizing temperature gradients.

3.2.4 Shell Structure

The shell, an "octahedral bucket," was manufactured from a single 144 x 25 cm honeycomb panel. By carefully cutting out a V-shaped wedge at seven equally spaced locations along the panel, one continuous piece of honeycomb could be "folded" into an octagonal shape, resulting in only one seam. These eight panels equal the sum of the lengths of the individual sides. This turned the honeycomb into 43.45 cm diameter regular octagon with an overall volume of 58,657.5 cm^3 (2.07 ft^3). The original design called for eight single panels 18 x 25 cm, which were joined to form an octagon. These joints were problematic at best. Each joint introduced localized stress concentrations that required massive mechanical over-building in the form of cover slips, through bolts and epoxy – all in an effort to transfer shear loads between face sheets. Even if these mechanisms provided the load transfer required, they would have added weight, and been more difficult to model, construct, and assemble than a continuous face sheet construction. Moreover, this method provides maximum transfer of shear stresses from each side.

The top plate is joined to the shell with eight angle brackets, one for each vertex of the octagon. Shur-Lock Corporation manufactured the honeycomb inserts used for anchoring bolts in the honeycomb.[11] Holes are drilled in the honeycomb exposing cells into which the inserts are placed. Space rated epoxy is then injected around the insert making it part of the spacecraft. The breadboard model uses stainless steel inserts since they will not gall easily with multiple use. The flight vehicle has little need for multiple access, but it was found that the security of steel could not be surpassed and steel inserts will be used on the flight model, the inserts have a specially deformed thread to keep the fasteners from backing out.

3.2.5 Tray

The trays are designed to support the subsystems during launch and provide a platform for the mission objectives. They are modular in nature and will allow for easy mounting and access. The trays are cut from a single sheet of aluminum honeycomb. The sides of the two inside trays (power tray and payload tray) will not be sealed off, as the shell will enclose them. Each shelf will rest on aluminum spacers, which separate the individual trays (Figure 3.11). The aluminum spacers will transmit loads through the structure and to the LVA. Each shelf will be 16.11 in (40.92 cm) long by 12.10 in (30.73 cm) wide, with a 2.71 in (6.89 cm) cutout oriented at 45 degrees to each corner. This will allow at least a 0.39 in (1 cm) drop clearance between the tray and the shell on all sides.

Figure 3.11: Modular Tray with Spacers

3.2.6 Spacers

The spacers are milled from a single piece of solid aluminum to a 3.95 in (10.03 cm) length, 0.251 in (0.64 cm) inner diameter to 0.55 in (1.4 cm) outer shaft diameter, and finally with a 0.16 in (0.4 cm) thick flange on each end at a diameter of 2.08 in (5.28 cm). The flange is offset from the end by the thickness of the trays, which is 0.5 in (1.27 cm). In this way, the spacers connect to the trays in the classic male (spacer) to female (tray) connection. A tight fit tolerance of 0.004 in (0.1 mm) between the hole and the spacer will help limit the wobble in vibration. Moreover, the through rods provide enough compressive force to keep the spacers aligned and stable throughout all aspects of loading.

The spacers are required to perform two important tasks. The first is to separate the trays and provide structural support for the satellite. The second is to provide a thermal conduction path between trays and out to the radiative FOSR material.

The spacers' primary function is load transfer. The four, ¼" rods alone could handle the on-orbit deployment load (310 lb_f), but not the larger (transient) loads associated with launch. Moreover, thermal subsystems require a minimum force of 1500 N for a good thermal transfer between spacers and trays. This compression force distributed across the width of the flange protects the honeycomb from localized bending. The 0.55 in (1.4 cm) central diameter provides plenty of strength to withstand compression, however, flange size varied widely depending on the core type of the aluminum honeycomb used (Figure 3.12).

Figure 3.12: Spacer Flange Diameter vs. Honeycomb Type

The flange diameter was determined by the equation:

d= (3-2)

Derived from classic, 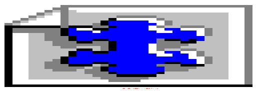

where, 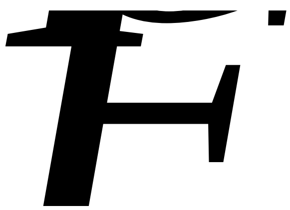

As the flange sizes differed, the spacer mass also varied (Figure 3.13):

Figure 3.13: Spacer Mass vs. Flange Radius

Bare Compressive Strength (5052, ¼ cell size, .0015" gage) = 240 psi (minimum)
(Ref: "5052 Alloy Hexagonal Aluminum Honeycomb - Specification Grade" chart on page 13 of TSB 120, Mechanical Properties of Hexcel Honeycomb Materials, Hexcel Corporation)

Based on this data, a flange diameter of 2.08 in (5.28 cm) was chosen which minimized mass, provided tray stabilization, and provided a minimum factor of safety of at least 1.4. The short analysis below shows a factor of safety above 4.

Flange Area = 3.393 in^2

Largest Force (deployment, pre-load torque, axial thrust) = Axial Thrust Load (8-12 Gs)
= 12 * 66 lb.
= 792 lb.

Axial Stress per flange = 58.36 pi

Factor of Safety = 240/58.36 = 4.1

Overall, this design allows for ease of assembly and modularity for development and troubleshooting, while maintaining the structural integrity of the superstructure. This spacer design provides the added benefit of enhancing the thermal conduction paths between trays and the outside radiators.

3.2.6.1 Spacer Thermal Function

Individual subsystem temperatures can vary widely due to constant change in thermal conditions such as during earth eclipse of the sun, operational cycling of various payloads, and the particular aspect angle a subsystem has with the sun. Significant thermal gradients can develop causing unwanted effects from the buildup or lack of heat in critical areas. Good thermal management is directly related to optimal performance, especially in the functionality of the batteries. Batteries that get too cold produce less power, and those that get too hot suffer from chemical breakdown, limiting their design life. Overall, subsystems that exceed their design temperature ranges and undergo large temperature gradients inevitably suffer performance losses and degrade rapidly.

The Thermal Subsystem detailed explicit requirements for the spacer design in order to achieve efficient thermal conduction. The main driver was to limit the number of discontinuities along a conduction path by limiting the number of contact surfaces between heat source and radiator. In order to help limit these discontinuities, each spacer was machined from solid aluminum. This limited the discontinuities to four contact points between the power (middle) tray and the outer radiating surfaces of the satellite (power box-tray-spacer-top/bottom plate-Solar Panel/FOR; each dash indicates a contact point.)

For an adequate thermal path, the contact area between the spacers needs to be maximized. In order to maximize the contact area, the central diameter must also be maximized. The original design called for a central diameter of 0.75 in (1.9 cm). The spacers, being milled from solid aluminum, had a mass of 4.18 lb. (1.9 kg). Since the mass conservation is important, optimizing the central diameter was critical. A range of diameters was examined to see their effect on overall mass (Figure 3.14).

Figure 3.14: Total Spacer Mass vs. Central Radius

An outside diameter of 0.55 in (1.4 cm) (diameter thickness = 0.77 cm) allowed for an adequate thermal path while maintaining structural rigidity and keeping individual spacer mass reasonable at 66.1 grams (actual = 70.1 grams). Actual mass deviation after machining, tolerances can vary up to 4 grams.

3.2.7 Component Placement

Top Plate

Camera Box

Shell

Spacers

Payload Tray

Power Subsystem

Power Tray

Hysteresis Rods

Spacers

Computer/Communications Subsystem

Computer/Communications Tray

Launch Vehicle Adapter

Figure 3.15: Component Placement

Each subsystem was assigned a place within the satellite based on volume, thermal and mission requirements. Balancing these requirements, and the desire for simplicity, resulted in each subsystem having its own tray. Refer to the figure on the left.

The top tray contains the experimental payloads: CCD camera, and the Micro Meteorite Impact Detector (MMID). The middle tray has the battery packs (boxes), the power relay switching and the control hardware. Power equipment placed on an isolated tray not only improved simplicity but limited other sensitive components (i.e. computers, experimental payloads) to direct exposure of radiant energy generated during the power system's charge/discharge cycle. Finally, the bottom tray supports the on-board computer and ham radio transceiver.

Of particular note in the design phase was the trade made between structural stiffness, load transfer, uniform thermal profiles, and favorable mass moments of inertia for attitude control. Batteries were originally located on the bottom tray to minimize transmitted structural loads and provide a short heat transfer path to radiative surfaces. This location was quickly revised after moment of inertia considerations revealed that the plane about the geometric center, or X-Y plane, was the preferred location. This placement maximized I_{zz}, while leaving the I_{xx} and I_{yy} essentially unchanged. To offset the location change, battery packs (boxes) were now milled from solid aluminum and enlarged to the height of a spacer; which proved beneficial in two ways. The boxes now served as spacers for tray separation; in fact, the load capability increased due to the greater overall surface contact area of the boxes as compared to the spacers. Likewise, the increase in contact area increased the overall thermal conductivity between the batteries and trays above and below the boxes. This turned out to be an important design discovery. The unfavorable moments of inertia were lowered (I_{xx} and I_{yy}) while maintaining the ability to quickly dissipate the batteries' high heat production and alleviate any concerns about heat buildup, and thus battery degradation (more on this in the Thermal Subsystem section). Accordingly, the relatively light computer/communications subsystem was moved down to the bottom tray. The end result was a "favorable" MOI, high I_{zz} relative to I_{xx} or I_{yy}, one in which the z-axis was the "favored" spin axis.

3.2.8 Antenna System[20]

Antenna Design/Tape Measure Housing

This design is different than any design previously considered. In this design the antenna is rolled on a spool that rolls freely on an axle of the housing, see figure 3.16.

S] Axel

Figure 3.16: Tape Measure Housing

The design is similar to the tape measure housing with the only difference that the tape is forced out by the spring inside the housing instead of pulling in as a conventional tape measure does. The design failed its initial tests, since the magnitude of the friction force was above predicted parameters. Furthermore, a spring with large spring constant will be needed to pull the antenna out of the housing. In order to reduce the friction - rollers need to be introduced along the inner radius of the housing. Figure 3.17: illustrates the placement of the rollers. Adding rollers complicated the design.

Figure 3.17: Roller Placement

Time will be required to design the precise location and selection of the rollers. The surface of the rollers should exert very low magnitude of resistance on the surface of the antenna in order to roll out of the housing with least amount of force. Due to time limitations, considerations of this design have been terminated.

Lesson learned from previous designs experience and other restrictions for a reliable design can be summarized:

1. The overall size of the antenna housing should not exceed 2.0 x 2.0 x 1.5 inches.
2. The base of the housing should not touch the solar panels.
3. When deployed, the levels should not hit the solar panels.
4. The power consumption should be low enough not to affect other subsystems.
5. The antenna should be rigidly held within the housing.
6. The material of the housing should not out gas or deform.
7. The force of the activation of the housing should not change or cause a significant moment on the satellite.

8. The friction between the antenna and the housing should be low enough to use a spring with a low spring constant.
9. The design should deploy the antennas at the specified orientation of 45 degrees from the z-axis.
10. The base plate should accommodate the pre-positioned and pre-selected screws on the satellite.
11. The aluminum housing should not cause an Electromagnetic interference with the antennas.

Spring Loaded Scissors Style Antenna Deployment Mechanism

The following design is the result of all the lessons learned from the previous design abiding by all the constraints posted by the others subsystems. Figure 3.18 shows a three dimensional representation of the new Antenna Deployment Mechanism.

Spring Le\Antenna

Figure 3.18: Antenna Deployment Mechanism

It consists of two levels that are equipped with three groves. The antenna is stowed to a certain diameter that fits into these groves that hold the antenna into a desired position. A torsion spring is introduced at the rotational axis of the level and the bottom plate of the mechanism. There are two torsion springs for two levels. The levels are held into position by a pin mechanism discussed later.

The unit is made of aluminum. The outer radius is 1.7 inches in diameter. The surface plate is 0.08 inches thick. This design has passed the initial test, i.e. the antenna is successfully deployed when the housing is opened. The antenna housing has been activated sixty times and it only failed eight times. Vibration, vacuum/thermal test procedures are in progress and actual tests will be conducted within one month.

This design has taken all constraints listed above into consideration. The following is a step-by-step discussion of each constraint qualified by the design.

The overall size of the antenna including the base is 1.7 x 1.7 x 1.2 inches. The two levels of the antenna are mechanically restricted by a restrain that does not allow the level to exceed more than 45 degree, thus protecting the solar panels beneath. The distance between the housing and the solar panel is only 0.1 inch. The fully deployed housing will shadow the solar panels, thus restricting the sunlight on the panels. However, the shadowing of the panels will not cause a drop in output efficiency, since the satellite is spinning and therefore the shadow will not stay on the panels for more than few seconds.

As shown in Figure 3.18 the antenna is placed between three evenly placed grooves on the level so that during the vibrations the antenna should not curl into a shape that would restrict the housing to deploy.

The base of the housing is aligned 45 degrees pointing away from the satellite, illustrated in
Figure 3.19.The housing is held to the top plate using a bolt that also holds the top plate to the shell of the satellite. A single bolt can cause the base to rotate due to vibrations. To restrict the rotation of the base a tack is introduced that runs though the base and the top plate of the satellite. The levels of the housing are spring activated which causes a downwards reaction during activation. However, the downward reaction caused by the housing on the top plate is small in

magnitude and it is canceled by the downward reaction of the housing on the bottom plate of the satellite. Therefore the reaction caused by all eight antennas housing cancel each other and does not cause a moment to the satellite. Figure 3.19 shows location of antennas.

Z-axis

Figure 3. 19 Antenna Position

3.2.9 Grapple System

Design and Requirements

The solar arrays must not be in contact of anything and the satellite must remain completely clean during its launch vehicle integration. Weighing roughly 90 lbs, a Grapple System is required to manipulate Spartnik.

Spartnik needs to be manipulated during its integration procedure, its transportation and its integration onto the launch vehicle. The grapple system was designed to meet the following:

- Enable two persons to handle the satellite along with the LVA
- Enable to safely move Spartnik with six degrees of freedom
- Deduce excessive deformation of the top plate that could break the top solar panels
- Be easily removable

Considering the shape of Spartnik, the idea to have a two-part device was proposed. The Grapple System will consist of a top handle and a bottom handle.

The design was done with the most valuable help of Ray Brindos from the machine shop and Prof. Victor Vagliente from the Civil and Environmental Engineering Department. The structural calculations where done by Prof. Vagliente.

Top Handle

The top handle consists of a ring attached to a square base plate through four grips. The four through rods that run through Spartnik represent the strongest points to attach the grapple system's top handle. Hence it was decided that the base plate of the top handle would be screwed with nuts to the protruding end of the through rods on the top plate of Spartnik.

The width of the ring is wider than Spartnik to protect it from any contact as well as applying a manageable torque during manipulations. The circular design allows easy handling of Spartnik at any position around its Z-axis as well as rotation around the Z-axis.

Bottom Handle

The bottom handle consists of three equally designed clamps to "hold" each of the three stand-off plates on the LVA. The handle is designed to enable access to the release mechanism, if needed, of the LVA. It also leaves freedom, of the manipulator, from any solar arrays and the launch vehicle itself.

In order to be able to easily and quickly remove the clamps from the stand off plate, quick release pins will be used.

Remaining Tasks

- The quick release pins and the nuts should be purchased.
- The Grapple system must be tested with Spartnik's prototype weighing at least 90 lbs. The test should verify that:
    - 2 persons can safely manipulate Spartnik using the Grapple System
    - The Grapple System is able to sustain the constraints
- Documentation should be written about this test to be included in the Safety Document
- The quick release pins and the nuts should be attached to the Grapple System with small chains so there is no hazard of dropping a piece in the launch vehicle during the integration. This will be fully described in the Spartnik Integration procedures (SIP)

3.3.0 Preliminary Design Analysis

Structural analysis was performed on the basic structure to help quickly eliminate inadequate designs. A finite element code called Mechanica, by Parametric Technologies Corporation, helped further to quickly optimizes the resultant structure. Preliminary design studies included various geometric shapes: cubic, pentagonal, hexagonal and octagonal. All geometries were modeled using identical loads. In the end, all geometries proved strong enough to withstand the anticipated loads, with the cubic shape being the strongest.

Extensive modeling was performed to confirm the viability of preliminary design ideas for the main satellite bus. All facets of the main bus were modeled to ensure their structural integrity during launch. Keep in mind, this preliminary analysis concentrated only on analyzing the shell and basic interior structure layout (i.e. trays). Thus, the following sections address only to analysis done on the basic superstructure, and only on Spartnik. The final design and analysis section discusses the finite element analysis results for the combined LVA/Spartnik structure.

3.3.1 Stiffness Matrix

Since honeycomb panels are orthotropic, it was necessary to input material properties for each type of honeycomb tested. Mechanica models these materials based on a given set of properties. These properties can be derived from the stiffness matrix, a series of equations[13] where each equation represents a different entry in the overall stiffness matrix (abd matrix).

$$\textbf{abd} = \begin{vmatrix} \textbf{A} & \textbf{B} \\ \textbf{B} & \textbf{D} \end{vmatrix}$$

where

n

(3-3)

$0 \quad _i \quad [$

(3-4)

[redacted]

(3-5)

(3-6)

Equation Reference: Introduction to Aerospace Structural Analysis. Allen, David H. and Walter E. Haisler. John Wiley & Sons Inc, Canada, 1985, p 111, equation 3-36.

This allows for the properties of all the material to be taken into account. Using these equations, a MATLAB[14] file was created to generate an 'abd' stiffness matrix of any material desired (Appendix 3E). These calculations were repeated in ADVLAM[15]. With the 'abd' matrix calculated, the flexibility matrix is obtained by taking the inverse of 'abd'. From here the Young's Modulus (E), Poisson's Ratio (v), and shear modulus (G) can be calculated for the three orthogonal axes of the material.

E1=1/abd(1,1) v1=-E1*abd(2,1) G1=1/abd(4,4)

E2=1/abd(2,2) v2=-E1*abd(3,1) G2=1/abd(5,5)

E3=1/abd(3,3) v3=-E2*abd(3,2) G3=1/abd(6,6)

These values are then loaded into Mechanica to provide the material characteristics of the honeycomb panels.

3.2.8 Static Load Constraints

Geometric models were made of each set studied which incorporated the calculated material properties, then the model was constrained such that it simulates a Launch Vehicle Adapter connection, and loads were placed upon it.

Table 3.4: Constraint Sets

Set 1	Fixed at the four through holes for the spacers and through bolts
Set 2	Fixed at the bottom edges
Set 6	Fixed at the bottom flange through hole
Set 8	Fixed at the bottom surface
Set 9	Fixed at the bottom surface

Table 3.5: Load Sets

Set 1	15 G acceleration in the minus z direction
Set 6	1500 N (337.2 lb_f) tension pulling orthogonal to each through hole
Set 8	15 G acceleration in the minus z direction & 1500 N (337.2 lb_f) Compression
Set 9	15 G acceleration in the minus z direction & 1500 N (337.2 lb_f) Tension

The Mechanica Analysis verified that the structure would not yield or deflect significantly under defined loads. The analysis also showed that the maximum stress level was at least one order of magnitude below the yield strength of the chosen material. Also, the maximum local deflections were insignificant ~$7.6x10^{-5}$ m. Appendix 3D shows the preliminary models on key components during the preliminary design. This finding permitted the design to proceed with the shell configuration. Furthermore, the detailed Finite Element analysis performed on the completed prototype is discussed in the following sections.

3.2.9 Transient Loads

The Preliminary Mechanica analyses indicate that high acoustical loading is the primary design constraint during the launch. These loads are commonly 50 Gs rms, in all axes, over a broad range of frequencies. The satellite must be designed to withstand these random launch loads while avoiding the natural frequency of the launch vehicle. The material, configuration, and dimensions had been defined, and were included in this preliminary (Mechanica) model. In addition, the stiffness matrix for the honeycomb material was added to refine the model, accounting for the honeycomb's isentropic properties. The results indicate that the shell design will withstand loads of 14 Gs in all axes, and more than 50 Gs in the primary directions.

Mechanica illustrations and modeling based on this preliminary modeling of the satellite are included in the Appendix 3D. In the final design and analysis, point masses will be added to the satellite model representing the different component masses and their location.

3.2.10 Modal Analysis (Spartnik only)

Two different runs were completed, within Mechanica, to analyze the expected enviromment the satellite will encounter. The two runs were identical for all four launch vehicles. These runs were the modal and static analyses. With the modal analysis, the boundary conditions for the first case included a 10% convergence of the element equations, a calculation of the first six modes and a polynomial order of nine for the element equations. The results indicated the frequency of the first mode fell at 42 Hz. This is right on target, as acoustic loads in the 40 Hz range is around 20 Gs. Thus the structure, which is designed to 50 Gs will survive in an 'average' launch enviromment. Further results are included in Appendix 3D.

3.2.11 Static Load Analysis (Spartnik only)

With the static analysis, the boundary conditions were also a 10% convergence on the element equations and a polynomial order of nine for the element equations. The maximum Von Mises stress was 3.1889E+6 Pa (462.4 lb_f), which is one order of magnitude smaller than the expected yield strength. The maximum displacement was 7.8790E-2 cm, which are two orders of magnitude less for the honeycomb. Further results are included in Appendix 3D. Overall, this preliminary analysis indicates that the satellite will not have any detrimental yielding or failures due to the expected sustained launch loads.

3.2.12 Final Design Analysis (Spartnik/LVA Combined)

The final design computer analysis must include the entire satellite and launch vehicle adapter combined as a system to adequately define what it will do as a whole. This is of particular concern to the launch vehicle manufacturer because they are most concerned of how the Spartnik system will behave and interact with their launch vehicle as well as the other payloads on board.

This computer analysis consists of dynamic loading to bring out the natural frequencies of the system and also specific static stress loading that simulates expected launch load scenarios. The dynamic loading will verify the systems natural frequencies so that they can be compared to launch vehicle resonant frequencies and the static loads will help in determining if the system is rigid enough to survive launch and orbital insertion.

3.2.13 Static Load Analysis / Constraints[1 8]

During launch, the spacecraft is subjected to high acoustical loads. The acoustic environment generates random vibration loads due to the noise pressure acting on the surfaces of the satellite. These loads are commonly 50 Gs over a broad range of frequencies. The satellite must be designed not only to withstand these random launch loads while avoiding the natural frequency of the launch vehicle, but also to protect the other systems from the major mechanical loads. Once the satellite is in orbit, the loads will be much lower than those during launch.

The static analyses of Spartnik were performed using the ANSYS commercial finite-element analysis computer code. Two different models were completed to analyze the expected environment the satellite would encounter. The reasoning for the two models is the same as those stated in the dynamic analyses. In general, the static model was the same as the dynamic model but with some modification. More elements were added for structurally critical points. Six analyses, three analyses per each case, were performed for the static analyses.

Once a natural frequency is determined from a dynamic analysis the actual load can be determined from the PSD (Power Spectral Density) chart, which is provided by a launch vehicle company, based on the natural frequency of Spartnik.

3.2.14 Modal Analysis[1 8]

The satellite is subjected to significant mechanical loads such as axial loads and shock loads during launch. Axial loads are generated by acceleration from the launch vehicle during the launch. Shock loads are generated by events like rocket engine ignition or stage separation. These vibration loads occur only at specific frequencies. If these frequencies coincide with natural frequencies of the Spartnik, the satellite could tear itself apart from the highly induced resonance. Therefore, frequency analysis of the structure is vital to its survival in the launch environment for safety reasons, natural frequencies of all payloads within a launch vehicle must be determined.

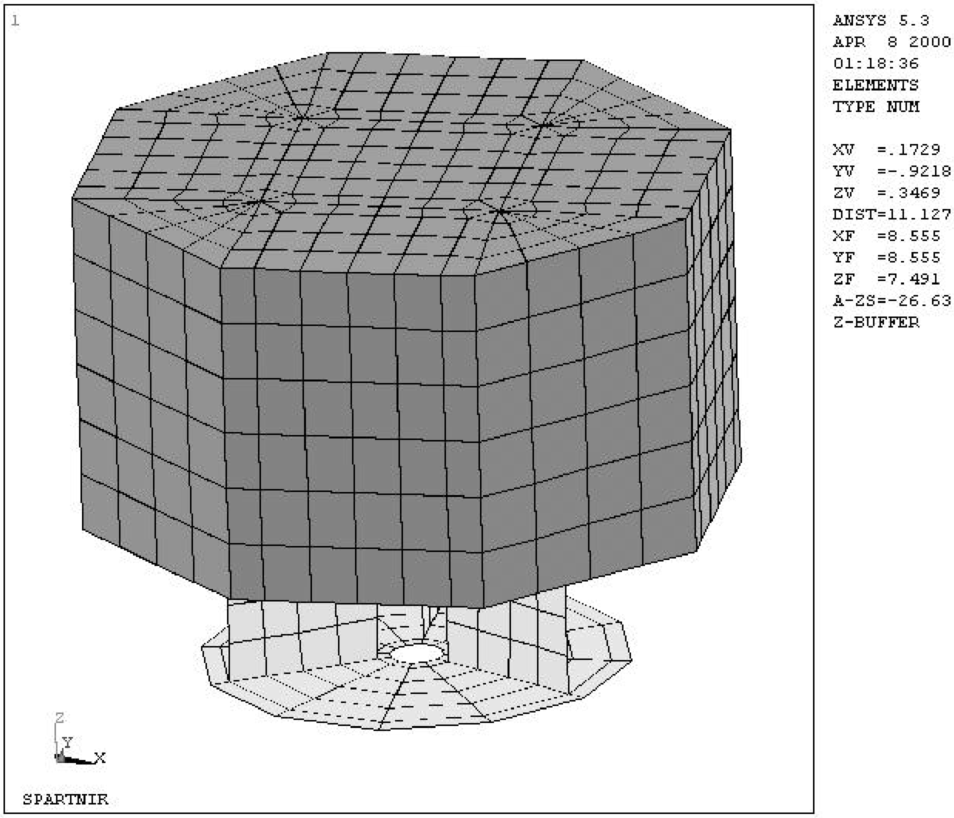

Figure 3.20 Overview of Finite-Element Model

The dynamic analysis of Spartnik presented here was performed using the ANSYS commercial finite-element analysis computer code. Mode shapes and frequencies were calculated in ANSYS using the Block Lanczos method. It was decided to determine all frequencies up to 20 modes to compare the ANSYS results with the other FEA results. This will be discussed more in the actual document. Two different runs were completed to analyze the expected environment the satellite will encounter. The reason for the two analyses was due to the contact points between the bottom plate and base plate. These two plates were attached with through rods at four points. The first analysis (Case One) was performed regarding these two plates as one plate; the bottom plate and base plate were modeled using the same elements. The first frequency, which was 123.3 Hz, of the result of the first analysis was little bit higher than expected value of around 70 Hz. After reviewing the original drawings of Spartnik carefully, a conclusion was made, that modeling two plates as one caused a higher frequency than expected. In the real environment the bottom plate and base plate will almost act like one piece but not ideally. The second analysis (Case Two) was performed after separating one plate into two plates; the bottom plate and base plate were modeled using two different types of elements. Unlike Case One, the bottom plate and base plate were only connected at each through rod hole.

3.2.15 Transient Analysis[1 9]

Once the accelerations from the launch vehicle have been recorded, they are incorporated into an input deck for application at the base of Spartnik (the attachment point between Spartnik and the launch vehicle). A transient analysis is run and accelerations gathered at critical points on Spartnik. The data points chosen were:

1. Communications Tray
2. Top Honeycomb Panel
3. Side Panel (1)
4. Side Panel (2)
5. Base Plate
6. Camera

Since the payload trays inside Spartnik are not square and will stiffen the sides of Spartnik uniformly, two side panel points were chosen. The accelerations are divided by the gravitational constant (386.1 in/s^2) before being plotted so that an easily visualized unit of 'g' can be used. Note that all accelerations are in response to normalized input loads and will therefore be a fraction of the actual responses. A detail representation of this can be seen in the actual document.

Section 3.2.15 through 3.2.18 will be completed using the Mechanica model of Spartnik imported into Pro/E. The Mechanica module in Pro/E will allow all facets of analysis: FEA, static and dynamic simulations with various loads. Computers at San José State University now have the capability to render such analysis with very high accuracy.

3.2.16 Mass Moments of Inertia and Products of Inertia

Moments and products of inertia of the satellite were calculated in two ways and compared for reasonableness. First, each component's mass was weighed and its distance measured from the top surface of the bottom plate at the intersection of vertex 5 (see the Figure 3.21).

It is important to note that the initial spacecraft design did not include the LVA, and thus special accommodations were made in the later stages of production to compensate for the LVA integration. The modifications included a plate attached to the lower side of the satellite namely side 10. This addition threw off the initial calculations for the moments of inertia. To compensate for the loss of control on the moments of inertia, special "mass enhancers" were added to the inside walls of the satellite shell. These mass enhancers bring back the relative magnitudes of the MOI.

Figure 3.21: Reference Origin

To

simplify the calculations, each component's mass was assumed to center around its geometric center. This assumption was acceptable since most components had a nearly even mass distribution. Applying the parallel axis theorem, the vehicle's overall moments of inertia were calculated. This was done along each axis. Products of inertia were found in the same fashion. The following is a list of the simplifications and assumptions used to calculate the Moments of Inertia (MOI) and the Products of Inertia (POI).

1. All components' locations were measured from a standard reference point.
2. All components are assumed homogeneous such that mass can be considered concentrated at the component's center of mass (geometric center).
3. All masses were measured at the component level or below (see spreadsheet in Appendix 3.F)
4. Placements of individual payload modules are approximated. (best estimate)
5. All mounting hardware is accounted for, however, the use of RTV or epoxy in the final steps of assembly is not accounted for.
6. The following components were not accounted for since the actual components have not yet been procured and/or developed: (wires, cables, connectors, etc.).

Based on these assumptions and the methods described above, an Excel spreadsheet was developed to help facilitate the calculations. A second method using a finite element code was used to corroborate these results. Spartnik was modeled in this FEM code using the same component weights and relative placement as done in the spreadsheet analysis. This FEM analysis should show strong correlation with the Excel spreadsheet and the results shown below for the FEM are for the satellite shell, trays, spools, threaded rods, satellite baseplate, and standoffs. Eric Abrahamson is currently helping the Structures Team to finish refining the model and will add the rest of the internal components to better match the results of the Excel Spreadsheet. The Table below summarizes the current results of the two methods and once refined the relative error between them should be calculated. [The moments of inertia as calculated through the Excel spreadsheet can be found in Appendix 3.G, and those calculated through FEM analyses can be found in Appendix 3.T.]

Table 3.6: Moments and Products of Inertia

INERTIA	MOIs			POIs		
	I_{xx}	I_{yy}	I_{zz}	I_{xy}	I_{yz}	I_{zx}
Excel Spreadsheet (kg*m^2)	0.15165	0.19897	0.26783	0.00009	-0.00044	-0.00315
FEM Analysis (kg*m^2)	0.0007683	0.0006950	0.000771	-1.98×10^{-7}	-6.95×10^{-8}	5.06×10^{-7}
Error (%)						

Ideally, I_{zz} should be large relative to the other moments of inertia and all the products of inertia would be nearly zero (to 10 decimal places). This ideal condition would guarantee that once spun about the Z-axis, Spartnik would then continue to maintain that orientation even with small perturbing forces (i.e. micro-meteorites). The results of the spreadsheet do not coincide with the results of the finite element code thus the calculations using the spreadsheet must be reconsidered and the error rectified.

3.2.17 Mass Budget

A mass budget satisfies two objectives: (1) insures that the launch vehicle requirement for secondary payload limit is not exceeded; and (2) it facilitates moment of inertia studies since relative weight contributions (and their location) can be easily assessed.

The overall limit set by the launch vehicle contractors for secondary payloads is 110 lbs (50 kg). Our design limit for Spartnik is 60 lb. (27 kg) plus an additional 10% weight margin (6.6 lb. or 3 kg), or a total of 66 lb. (30 kg). We are well within our weight budget (currently at 55 lb). The Excel spreadsheet (filename: finerbal.xls, see Appendix 3G) gives the details of the individual component weights. The major weight item that still needs to be developed and assembled for Spartnik is solar panels. Nevertheless, we do not anticipate exceeding the design limit.

Some items, like wires, connectors, etc., have not yet been accounted for, but they should contribute little in proportion to the overall mass and thus, this analysis is still adequate for assessing weight budgets and overall MOIs until a more accurate assessment can be made. Included however, are the mass enhancers, which were designed and integrated to help the spacecraft's spin in orbit. The moments of inertia, which are meant to stabilize the satellite across the z-axis, need Izz to be the dominant between Ixx and Iyy.

An updated spreadsheet of components arranged by subsystem is included in the appendix. This six-part list was review on March 1998, and includes, in addition to the mass budget, calculations of the center of mass, and moments of inertia for each structural component.

3.2.18 Manufacturing Requirements

Integral to maintaining low cost development on any project is insuring ease of assembly and high modularity. In addition, in-house resources or donated shop time (students or industry) were implemented as much as possible.

Strict tolerances are critical for proper alignment especially during the development phase with multiple cycles of assembly/re-assembly and fit checks. The honeycomb portions of the satellite were machined by computer numerical control (CNC) methods using automated vertical milling equipment. CNC allows for tight tolerances throughout the part.

The assigned tolerances were 0.0002m (0.008 in) for all components. Because of the number of parts, and the requirement for modularity, tight tolerances and consistency throughout, all cut angles and hole locations were critical. All components need to adhere to tolerance requirements to assure accurate assembly.

Fortunately, for the production of the flight model, the structures team has Ray Brindos and his team of technicians producing 90% of the parts. Ray is a San Jose State employee working for the Engineering department. Ray produces high quality parts, which will make for a well fitting throughout the satellite.

3.2.19 Manufacturing Milestones Currently Achieved

Spartnik shell

The shell interior has been fitted with mass enhancers, permanent magnets and coated with space rated thermal paint. Solar cells have been applied to the exterior thanks to the work of Mike McCormick and the shell is currently under testing to determine if the solar arrays are functional. Once testing is complete the shell will be returned to San José State University.

Top and Bottom Plate

The top plate has been fabricated after minor adjustments. Inserts have been installed and the bottom of the top plate has been coated with space rated thermal paint. The bottom plate has undergone modifications to its final design, which reflects the requirements of the micro-switch and umbilical connector dimensions. It is currently at Lockheed Martin where solar panels have been placed and will be transported to our cleanroom before semester's end.

Camera: Box, Plate and Periscope

The redesigned box and plate have been fabricated as well as the mounting fasteners. The periscope design has been modified to reflect the new dimensions of the camera box and has been redrawn in Pro/Engineer.

Spacers

The spacers, which contact the top and bottom plates, have been modified to reflect the placement of inserts in the top and bottom plates. Modification included the removal of one of the protrusions at each end of the spacers.

Base plate

The base plate has been redesigned. The modifications to the base plate include the dimensions of the micro-switches and the umbilical connector.

Nutation Damper

A prototype of the nutation damper has been made using a brazing technique to fuse the two ends to form a circle this was found to be a more robust design. A flight model is yet to be tested.

Antenna Deployment

A new antenna design deployment has been manufactured and will undergo testing and perhaps more modifications. The new design now employs a hood to secure the antenna and a spring release mechanism.

Launch Vehicle Adapter

Two thirds of the LVA is complete: standoffs, hub and LV base plate. Required are the bolting patterns for the specified launch vehicle, components for the release mechanism and a new spring with proper spring constant.

Grapple System

Manufactured to transport Spartnik onto the launch vehicle, the grapple system has been designed to attach to the LVA's three stand-off plates and to the top plate via the through rods.

Cleanroom

A cleanroom has been erected in ENG 236 in preparation for satellite integration and testing. The specifications for the cleanroom are noted in the Cleanroom Subsystem FDR.

Safety Document

A safety document has been prepared and will be undergoing changes as Spartnik progress towards integration. The purpose of the document will serve as a list of hazards that can affect Spartnik as well as the launch vehicle. Refer to the document for further details.

3.3 Construction/Integration

The Spartnik Integration Procedures (SIP) have begun but is not yet fully completed. The uncompleted version can be seen in its own document format. It has been distributed for review by sub-system leads where they will sign off as a witness to the integration.

3.4 Verification Testing

A complete structural verification test of Spartnik coupled to the Launch Vehicle Adapter has been performed. This test assures the launch vehicle contractor that Spartnik will maintain structural integrity from launch through on-orbit deployment, and that it will not inadvertently activate or deploy any of its systems that may endanger personnel, the launch vehicle, and other payloads. Spartnik has been tested under anticipated static and dynamic load environments simulating launch, ascent and space operations to verify survivability, functionality and safety.

Structural testing will be comprised of four major phases. These four tests will characterize the flight vehicle and verify computer modeling of natural frequencies and
displacements. The test phases are as follows:

- Sine sweep test. Determines structure's natural frequencies.
- Sinusoidal vibration at qualification and acceptance levels. Axial Loads
- Random vibration test at qualification and acceptance levels. Acoustical Loads
- Qualification shock test. Engine start and Stage separation.

The natural frequency verification test requirements vary by launch vehicle. The general consensus is that a frequency below 40 Hz is safe for most payloads. The loads for most launch vehicles at 40 Hz is approximately 20 Gs, which is well within the design limits of Spartnik. Spartnik is currently being computer simulated with random vibration loads of 50 Gs in all three directions.

3.3.1 Verification Test Overview

As discussed in the previous section, Spartnik and the LVA were tested as a single unit.
Spartnik/LVA was tested under the most stringent load environments as delineated by each launch vehicle reference guide (Ariane, LMLV, and Pegasus) for nominal operations during launch, ascent, and deployment Accelerometer locations can be found on the next page.

1. 0.5 G input sinusoidal vibration signature sweep
2. 10 G acceptance level random vibration
3. 14 G qualification level random vibration
4. 0.5 G sinusoidal vibration to recheck signature of satellite and LVA
5. 2000 G shock test performed over 120 ms

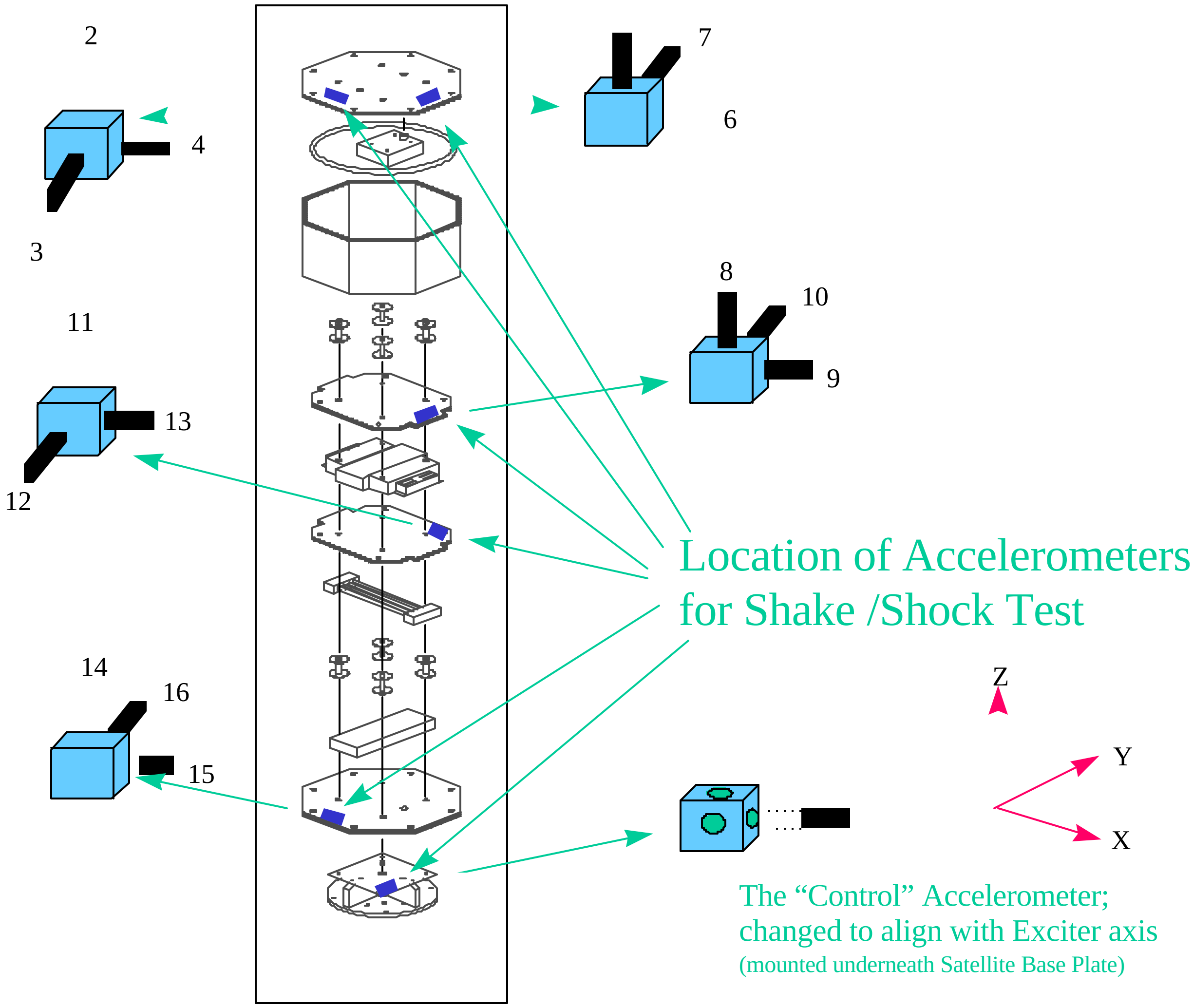

Figure 3.22: Accelerometer Locations for Shake Test

3.4 Operations

Not applicable until final solar array placement and integration of all the structural components into the flight shell.

3.5 Conclusions

We have made significant progress as far as the manufacturing phase is concerned. Great care has been observed in the selection and finalization of the CAD drawings for the several components. Some parts are still undergoing manufacture, and they are subject to time constraints and machine-shop specialist availability.

The review process has been made possible thanks to the collaboration of all other subsystems members involved, the participation of sponsors/mentors, and the final approval of this year's projects systems engineer. A detailed description of the major milestones achieved during the last semester and current status of manufacturing process follows:

1) Thanks to the collaboration of payload & power subsystem team leaders, we were able to finalize the camera box and accessories.

2) Complete manufacturing of the camera box has been achieved.

3) Proper measurement of flight shell side panels and solar array dimensions.

4) An improvised design of a drilling guide was necessary to properly locate and accurately drill holes for solar array placement onto the flight shell

5) Due to the fact that the company who volunteered to fabricate the solar arrays had some difficulties in regards to the dimensions, we had to compensate for the
previously drilled holes by filling the holes with space-rated epoxy.

6) Since solar array placement is a very complex and delicate process which we do not have facilities here at San Jose State University, we sent the flight shell to Lockheed Martin Missiles & Space Co. to accomplish this manufacturing/assembly phase.

7) Complete manufacturing of the Launch Vehicle Adapter (LVA) together with the standoffs was achieved. Revisions will be done per Launch Vehicle Specs, to ensure proper fit to Launch Vehicle.

8) Currently, we are working on a complete Finite Element Analysis (FEA) for each of the internal structural components of the spacecraft. We are utilizing SolidWorks? , which is software package that contains the Cosmos ? finite element analysis program, for the final integrated analysis of "Spartnik".

   Minor impediments arose due to lack of computer memory to run the analysis (currently is 215 Hz), and we are looking into simplifying the new analysis with a different kind of processor with a greater capacity.

9) Also, we are in the process of reviewing and implementing a new design for the spacecraft communications antennae. Several ideas have been explored, however, we are concentrating our attention in a design that will allow us to avoid rupture due to stress accumulation at the attachment bolts that hold the antennae to the brackets, which, in turn, remain fixed on the top z+ plate.

10) The finalization of the CAD drawings for the top z+ plate (which will carry the camera box, Micro Meteorite Impact Detector, and nutation damper) has been completed and now is in the course of being manufactured in the machine shop.

11) Finally, we have worked together with our mentor, Patrick Arriola, to verify the final modifications to the CAD drawings for the periscope, which is going to be lodged, once wrapped in the foam, in the interior of the camera box. We have arrived at a consensus and the periscope drawings have been completed and are currently being manufactured.

3.6Hysteresis bars

The elimination of the hysteresis bars will not cause major structural changes to Spartnik. See the ADAC FDR for why they were deleted from the design. It was concluded that eliminating them would be best for the function of the spacecraft since they could affect rotation about the non-principle axis of rotation. It is safe to structurally remove them with out fear of changing any of the fundamental characteristics of Spartnik for the following two reasons.

The structural analysis performed on Spartnik falls in to two primary categories. The first was a computational analysis performed using the computer program 'Pro Mechanica\mmotion'. The model used in this analysis did not include hysterisis rods. On the computer named 'Europa' the file path to these models is 'F:\users\jaehyungkim\spartnikXXX'.

The second structural analysis done on Spartnik was a vibration test performed on a full size mock up of the spacecraft. The physical model used did include some rods that represented the hysterisis rods but these rods were little more than coat hangers and would have played little part in the dynamics. The real hysterisis rods were to be considerably more massive. So in the physical vibration test effectively the hysterisis rods were not included. Therefore the flight vehicles dynamic performance will not differ significantly from the predicted response due to a lack of hysterisis rods.

References

1. Pisacane, V.,Moore, R.,Fundamentals of Space System, Oxford University Press, New York, 1994, P.477.
2. Pisacane, V.,Moore, R.,Fundamentals of Space System, Oxford University Press, New York, 1994, P.485.
3. Pisacane, V.,Moore, R.,Fundamentals of Space System, Oxford University Press, New York, 1994, P.552.

4. NASA, NASA Hitchhiker, Goddard Space Flight Center Greenbelt MD, copyright 1994, P.3-6.
5. Lockheed Missile & Space Company, Inc., Lockheed Launch Vehicle User's Guide, Sunnyvale, CA, copyright 1995, P.38.
6. OLS, Pegasus User's Guide, Virginia, Copyright 1991.
7. Aerospatiale, Ariane User's Guide.
8. TSB-120, Hexcel Corporation, copyright 1992.
9. TSB-120, Hexcel Corporation, copyright 1992.
10. Agarwal, B., Design of Geosynchronous Spacecraft, Prentice Hall, P.215, 245.
11. Shur-Lock corp., 2541 Whise Road, Irvine, CA, catalog 2.5m 9/93.
12. Mechanica Release 6.0, Rasna Corporation, San Jose, CA, copyright 1990-1994.
13. MIL-HDBK-5E, Metallic Materials and Elements for Aerospace vehicle Structures, P.1-9,1-10, copyright 1987.
14. Matlab, Mathworks Inc. 1992.
15. ADVLAM, LMSC-0812170, 1983.
16. Gere, J.M., Timoshenko, S.P., Mechanics of Material, 3rd ed., PWS-KENT Publishing Company, Boston, 1990, P.748.
17. Isakowitz, Steven J., International Reference Guide to Space Launch Systems, 2nd ed., published and distributed by American Institute of Aeronautics and Astronautics, 1995.
18. Kim, Jaehyung, Finite Element Analysis of Spartnik, May 2000.
19. Fowler, Emily Catherine. Finite Element Modeling and Analysis for the San Jose State University Student Satellite Program: SPARTNIK, May 2000.
20. Singh, Robbie. AIAA Student Conference Paper, Antenna Deployment System, May 2000.

Mentor List

Eric Abrahamson, Ph.D., Lockheed-Martin Space & Missiles Company, Sunnyvale, CA
E-mail: abrah@scsolutions.com

Jim Prass
E-mail: jimp@tandem.com
Phone: (408) 249-9539

Mark Mallinson, Mechanical Engineer, NASA-Ames
Phone: (415) 604-6322

Dave Himmelblau, Lockheed-Martin Space & Missles Company, Sunnyvale, CA.